Synthesis and characterisation of ruthenium(II) complexes containing ferrocenyl-derived ligands

Carla D. Nunes,[a] Teresa M. Santos,*[a] Helena M. Carapuça,[a] Alan Hazell,[b] Martyn Pillinger,[a] João Madureira,[a] Wen-Mei Xue,[c] Fritz E. Kühn[c] and Isabel S. Gonçalves*[a]

[a] *Department of Chemistry, University of Aveiro, 3810-193, Aveiro, Portugal.*
E-mail: igoncalves@dq.ua.pt.; Fax: +351 234 370084
[b] *Department of Chemistry, University of Aarhus, Langelandsgade 140, DK-8000, Aarhus C, Denmark*
[c] *Anorganisch-chemisches Institut der Technischen Universität München, Lichtenbergstraße 4,*
D-85747, Garching bei München, Germany

Received (in Montpellier, France) 24th April 2002, Accepted 7th June 2002
First published as an Advance Article on the web 9th September 2002

Ruthenium(II) complexes containing the macrocycle [14]aneS$_4$ and pyridyl ligands with an end-capping ferrocene were prepared using [Ru([14]aneS$_4$)(DMSO)Cl]Cl as the starting material. Substitution of the DMSO ligand by 4-ferrocenylpyridine (4-FP), ferrocenyl-4-pyridylacetylene (FPA) and pyridine (py) gave the complexes [Ru([14]aneS$_4$)(L)Cl]Cl (L = 4-FP, FPA, py). The acetonitrile complex [Ru([14]aneS$_4$)(NCMe)$_2$](BF$_4$)$_2$ was also prepared starting from [Ru([14]aneS$_4$)(DMSO)Cl]Cl. UV/Vis absorption spectroscopy and cyclic voltammetry indicate low electronic communication between the metal centres in the heterobimetallic complexes. The crystal structure of [Ru([14]aneS$_4$)(4-FP)Cl]Cl was determined by X-ray diffraction. Crystal data: $C_{25.780}H_{37.134}Cl_2FeNO_{1.288}S_4Ru$, $M = 737.82$, monoclinic, space group $P2/n$, $a = 13.192(1)$, $b = 7.6662(6)$, $c = 28.549(2)$ Å, $\beta = 100.341(2)°$, $V = 2840.4(4)$ Å^3, $Z = 4$.

Introduction

Since the discovery of ferrocene (Fc), numerous derivatives of the type Fc-X have been prepared.[1] In particular, ferrocenyl derivatives containing metal-binding moieties have been sought, with the aim of preparing heterobimetallic complexes. Ideally the two metal centres should be coupled through suitable unsaturated bridging units, in order to facilitate electronic communication. Changing the oxidation state of the pendant ferrocenyl unit may allow tuning of the electron density at the second metal centre without changing the immediate coordination sphere.[2] Ferrocene-based ligands are obviously good for these purposes because ferrocene-centred oxidations should be reversible. Considerable attention has been paid to aromatic N-heterocyclic ligands functionalised with ferrocenyl groups, for example pyridine,[2–6] 2,2′:6′,2″-terpyridine[7] and pyrazole.[8] The coordination capabilities of these organometallic ligands have generally been investigated by coordination to metal carbonyl fragments. For example, reaction of 4-ferrocenylpyridine (4-FP) with Re(CO)$_5$Cl gave the Re(4-FP)$_2$(CO)$_3$Cl complex.[2] Complexes of the type [(FP)Ru(NH$_3$)$_5$](PF$_6$)$_2$[4] (FP = 3-FP or 4-FP) and M$_2$(O$_2$C-R)$_4$(4-FP)$_2$ (M = Rh, Mo)[6] have also been obtained. Introduction of an acetylene linker in 4-FP gives ferrocenyl-4-pyridylacetylene (FPA),[9] which forms complexes with metal carbonyl fragments,[9] multiply bonded metal–metal complexes,[6,10] and methyltrioxorhenium.[11] Several other types of conjugated linkers have been employed, incorporating alkene, alkyne, and phenyl entities.[9,12–16] Ferrocenyl heterobimetallic complexes are being investigated with several potential applications in mind, including non-linear optics.[12,13,17] In this paper we wish to report on the reaction of the ligands 4-FP and FPA with the complex [Ru([14]aneS$_4$)(DMSO)Cl]Cl ([14]aneS$_4$ = 1,4,8,11-tetrathiacyclotetradecane), providing dinuclear complexes of the type [Ru([14]aneS$_4$)(L)Cl]Cl. The ruthenium(II) fragment [Ru([14]aneS$_4$)Cl]$^+$ readily incorporates monodentate N-donor ligands,[18] as shown also for other ruthenium(II) complexes containing the macrocyclic ligands [9]aneS$_3$[19,20a] and [12]aneS$_4$.[20b]

Experimental

General procedures and starting materials

Microanalyses were obtained with a LECO CHNS-932 Elemental Analyser. Thermogravimetric analysis (TGA) studies were performed using a Mettler TA3000 system at a heating rate of 5 K min^{-1} under a static atmosphere of air. IR spectra were obtained as KBr pellets using a FTIR Mattson-7000 infrared spectrophotometer. UV/Vis spectra were obtained at room temperature with a Jasco V-560 spectrophotometer. ^{1}H NMR spectra were recorded on a Bruker AMX-300 spectrometer.

Electrochemical measurements were performed using a BAS 100B/W electrochemical analyser controlled by BAS data acquisition software. Cyclic voltammograms were obtained at room temperature in deoxygenated 0.1 M tetrabutylammonium hexafluorophosphate (TBAPF$_6$) in CH$_2$Cl$_2$ or MeCN, with a conventional three-electrode cell. The working electrode was a Pt disc (geometric area 2.0 mm^2), the auxiliary electrode was a Pt wire and the reference electrode was Ag/Ag$^+$ (0.010 M AgNO$_3$ in 0.1 M TBAPF$_6$/MeCN). The reference electrode was calibrated against the ferrocene/ferrocenium redox couple (1 mM). In both solvents under study, ferrocene presented $E_{1/2} = +0.091$ V *vs.* Ag/Ag$^+$, with a peak separation, ΔE_p (anodic to cathodic), of 67–74 mV. All potentials quoted are related to the Ag/Ag$^+$ reference electrode. At the beginning of the experiments, the working electrode was polished with 1 μm diamond paste and 0.03 μm alumina slurry and rinsed

DOI: 10.1039/b204002f

with water and MeCN. Cyclic voltammetric scan rates ranged from 20 to 200 mV s^{-1}.

All preparations and manipulations were performed using standard Schlenk techniques under nitrogen. Commercial grade solvents were dried and deoxygenated by refluxing with appropriate drying agents under nitrogen and distilled prior to use. The compounds *cis*-$[Ru(DMSO)_4Cl_2]$,[21] $[Ru([14]aneS_4)(DMSO)Cl]Cl$,[18] $[Ru([12]aneS_4)(ind)Cl]Cl$ (ind = indazole),[20b] 4-ferrocenylpyridine[2] and ferrocenyl-4-pyridylacetylene[15] were prepared using modified literature procedures. Ferroceneacetonitrile (FA) was obtained from Aldrich and used as received.

Preparation of ruthenium complexes

Preparation of $[Ru([14]aneS_4)(4\text{-}FP)Cl]Cl$ (1). A mixture of solid 4-ferrocenylpyridine (0.13 g, 0.49 mmol) and $[Ru([14]aneS_4)(DMSO)Cl]Cl$ (0.25 g, 0.48 mmol) in dry ethanol (20 mL) was refluxed for 3 h. After concentration of the resulting solution to 5 mL and addition of diethyl ether (20 mL), an orange solid was obtained. The compound was recrystallised from ethanol/hexane (0.25 g, 75%) (Found: C, 42.67; H, 4.73; N, 1.99; S, 18.23. $C_{25}H_{33}Cl_2FeNRuS_4$ requires C, 42.43; H, 4.51; N, 1.82; S, 18.01%); Selected ν_{max}/cm^{-1} 3071 w, 2956 w, 2915 w, 1609 s, 1517 m, 1425 s, 1289 m, 1215 m, 1105 m, 1079 m, 1033 m, 1004 m, 860 m, 835 m, 816 s, 786 m, 642 w, 533 m, 485 m, 427 m, 377 w (KBr); δ_H (300 MHz, $CDCl_3$, $SiMe_4$) 8.52 (d, H_α of py), 7.34 (d, H_β of py), 4.73 (t, C_5H_4), 4.51 (t, C_5H_4), 4.10 (s, Cp), 3.72–3.64 (m, $[14]aneS_4$), 3.33–2.64 (m, $[14]aneS_4$), 2.24–1.91 (m, $[14]aneS_4$)

Preparation of $[Ru([14]aneS_4)(FPA)Cl]Cl$ (2). A mixture of ferrocenyl-4-pyridylacetylene (0.07 g, 0.24 mmol) and $[Ru([14]aneS_4)(DMSO)Cl]Cl$ (0.12 g, 0.24 mmol) in dry ethanol (20 mL) was refluxed for 12 h. After concentration of the resulting solution to 8 mL and addition of diethyl ether (20 mL), an orange/brown solid was obtained. The compound was recrystallised from ethanol/hexane (0.13 g, 62%) (Found: C, 44.36; H, 4.42; N, 1.83; S, 17.42. $C_{27}H_{33}Cl_2FeNRuS_4$ requires C, 44.57; H, 4.57; N, 1.92; S, 17.63%); Selected ν_{max}/cm^{-1} 3071 w, 2956 w, 2915 w, 2199 m, 1602 s, 1418 s, 1273 m, 1077 m, 1017 m, 1004 m, 913 m, 862 m, 821 m, 668 w, 550 m, 485 m, 426 m, 376 w, 302 w; δ_H (300 MHz, CD_2Cl_2, $SiMe_4$) 8.58 (d, H_α of py), 7.30 (d, H_β of py), 4.50 (t, C_5H_4), 4.28 (t, C_5H_4), 4.17 (s, Cp), 3.56–2.85 (m, $[14]aneS_4$), 2.76–1.69 (m, $[14]aneS_4$)

Preparation of $[Ru([14]aneS_4)(py)Cl]Cl$ (3). A mixture of pyridine (0.59 g, 7.4 mmol) and $[Ru([14]aneS_4)(DMSO)Cl]Cl$ (0.10 g, 0.19 mmol) in dry ethanol (10 mL) was refluxed for 3 h. After concentration of the resulting solution and addition of diethyl ether (20 mL), an orange/yellow solid was obtained (0.09 g, 90%) (Found: C, 34.82; H, 5.02; N, 3.00; S, 24.85. $C_{15}H_{25}Cl_2NRuS_4$ requires C, 34.67; H, 4.85; N, 2.70; S, 24.68%); Selected ν_{max}/cm^{-1} 2915 m, 1600 m, 1482 m, 1440 s, 1276 w, 1066 m, 1018 m, 860 m, 763 s, 698 s (KBr); δ_H (300 MHz, CD_3NO_2, $SiMe_4$) 8.80 (d, H_α of py), 7.93 (t, H_γ of py), 7.47 (m, H_β of py), 3.65–2.90 (m, $[14]aneS_4$), 2.85–2.35 (m, $[14]aneS_4$), 2.15–1.70 (m, $[14]aneS_4$)

Preparation of $[Ru([14]aneS_4)(NCMe)_2](BF_4)_2$ (4). $TlBF_4$ (2.19 g, 7.5 mmol) was added to a solution of $[Ru([14]aneS_4)(DMSO)Cl]Cl$ (1.3 g, 2.5 mmol) in MeCN (20 mL) and the mixture refluxed for 48 h. After filtration through celite, the solution was concentrated and the product obtained as a pale yellow powder by precipitation with hexane/diethyl ether (1.55 g, 98%) (Found: C, 26.61; H, 4.00; N, 4.06; S, 20.82. $C_{14}H_{26}B_2N_2F_8RuS_4$ requires C, 26.89; H, 4.19; N, 4.48; S, 20.51%); Selected ν_{max}/cm^{-1} 2932 s, 2284 w [$\nu(N{\equiv}C)$], 1437 s, 1425 s, 1412 s, 1304 s, 1278 s, 1240 m, 1078 vs, 920 s, 862 s, 828 m, 771 m, 576 m, 533 s, 521 s, 469 m, 357 m, 325 m; δ_H (300 MHz, CD_3NO_2, $SiMe_4$) 3.62–3.27 (m, $[14]aneS_4$), 3.07–2.61 (m, $[14]aneS_4$), 2.54 (6 H, s, NCMe), 2.42–1.97 (m, $[14]aneS_4$).

X-Ray crystallography

Crystal data for **1**: $C_{25.780}H_{37.134}Cl_2FeNO_{1.288}S_4Ru$, $M = 737.82$, monoclinic, space group $P2/n$, $a = 13.192(1)$, $b = 7.6662(6)$, $c = 28.549(2)$ Å, $\beta = 100.341(2)°$, $V = 2840.4(4)$ Å^3, $Z = 4$, $T = 120$ K, $\mu = 1.548$ mm^{-1}. A total of 29 728 reflections ($2.4 < \sigma < 29.8°$) were measured on a Siemens SMART diffractometer using graphite monochromated MoK_α radiation (0.71073 Å) yielding 5888 unique reflections (Rint = 0.040). Data were corrected for Lorentz-polarisation effects and for absorption.[22] Refinement (on F) converged at $R1 = 0.052$, $wR1 = 0.046$ ($I > 3\sigma I$). The structure is disordered. The cyclopentadienyl group, C21 to C25, is disordered over two sites, the two groups were constrained[23] to be identical regular pentagons, the radius of which was refined. The sum of the occupation factors for the two sites was constrained to be exactly unity. Anisotropic displacement parameters for both the cyclopentadienyl groups were modelled by T, L and S tensors.[24] The chloride ions which were originally located on 2-fold axes refined to give extremely anisotropic displacement factors and were modelled by pairs of half atoms. Solvent molecules were initially modelled as water but a difference map showed extra peaks close to the O2 site. The extra atoms were interpreted as ethanol, the sum of the occupation factors for the water and the ethanol was less than 1. Solution of the structure in lower symmetry space groups (Pn or $P2$) did not remove the disorder and yielded many non-positive definite displacement factors, hence the disordered solution in $P2/n$ was retained. Hydrogen atoms for the ligand were kept fixed in calculated positions with C–H = 0.95 Å and Uiso = $1.2 \cdot U$eq for the atom on which they were bonded, the hydrogen atoms belonging to the water molecules were neither located nor included in the calculations.

CCDC reference number 184371.

See http://www.rsc.org/suppdata/nj/b2/b204002f/ for crystallographic data in CIF or other electronic format.

Results and discussion

Preparation of ruthenium(II) complexes

It was shown previously that the coordinated DMSO ligand in the complex $[Ru([14]aneS_4)(DMSO)Cl]Cl$ can be readily replaced by donor nitrile ligands, namely acetonitrile and 4-(triethoxysilyl)butyronitrile, to give complexes of the type $[Ru([14]aneS_4)(L)Cl]Cl$.[18] In the present work we have used the same synthetic methodology to introduce monodentate N-donor ligands functionalised with ferrocenyl groups, with the intention of forming heterobimetallic complexes containing pendant ferrocenyl subunits. Initial efforts centred on using the readily available ferroceneacetonitrile (FA). However, reaction of $[Ru([14]aneS_4)(DMSO)Cl]Cl$ with FA in refluxing ethanol and in the presence of $TlBF_4$ did not give the desired dinuclear complex $[Ru([14]aneS_4)(FA)Cl](Cl,BF_4)$. It was thought that this was due to the poor solubility of FA in ethanol. Carrying out the reaction in ethylene glycol at 140 °C did result in the formation of a clear homogeneous solution but the solid isolated from this mixture was insoluble in common organic solvents and coordination of the ferrocenyl ligand was not supported by solid-state NMR studies and elemental analysis.

No further attempts were made with FA as the organometallic ligand. Instead, the ligands 4-ferrocenylpyridine and ferrocenyl-4-pyridylacetylene were prepared and reacted with $[Ru([14]aneS_4)(DMSO)Cl]Cl$ in ethanol. In both cases orange solutions were formed from which the products

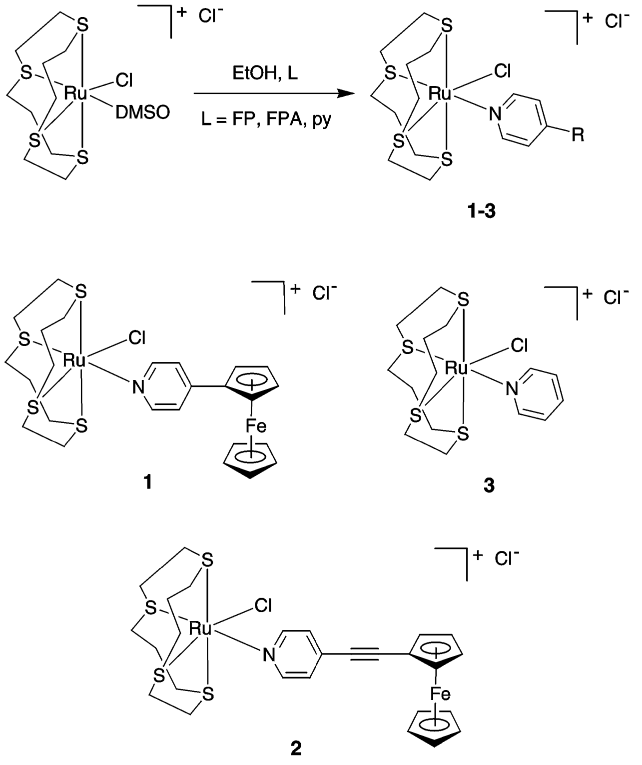

Scheme 1

[Ru([14]aneS$_4$)(4-FP)Cl]Cl (**1**) and [Ru([14]aneS$_4$)(FPA)Cl]Cl (**2**) were isolated as analytically pure crystalline solids in good yields (Scheme 1). The same method was used to obtain the pyridine adduct [Ru([14]aneS$_4$)(py)Cl]Cl (**3**). Compounds **1**–**3** are air stable and soluble in polar organic solvents such as acetonitrile and ethanol.

Coordination of the pyridyl groups in **1** and **2** to the ruthenium(II) metal centre is supported by ^{1}H NMR (measured in CD_2Cl_2 or $CDCl_3$) and FTIR spectroscopy (measured in KBr). Thus, the pyridyl resonances of **1** [$\delta(H_\alpha)$ 8.52, $\delta(H_\beta)$ 7.34] and **2** [$\delta(H_\alpha)$ 8.58, $\delta(H_\beta)$ 7.30] differ in their chemical shift from those of non-coordinated FP [$\delta(H_\alpha)$ 8.44, $\delta(H_\beta)$ 7.30] and FPA [$\delta(H_\alpha)$ 8.53, $\delta(H_\beta)$ 7.32]. On the other hand, the ferrocene proton resonances are largely unaffected compared to the "free" ligands, undoubtedly because they are distant from the Ru^{II} centre. Apart from the resonances for the organometallic ligands, the spectra of **1** and **2** display a series of multiplets in the range $\delta = 1.7$–3.7 for the protons of the macrocycle [14]aneS$_4$, similar to the pattern exhibited by the precursor [Ru([14]aneS$_4$)(DMSO)Cl]Cl.[18] In the IR spectra, the pyridyl ring stretches shift from 1598, 1594 and 1590 cm^{-1}, for the free ligands 4-FP, FPA and py, to 1609, 1602 and 1600 cm^{-1}, for the adducts **1**–**3**. In the case of [Ru([14]aneS$_4$)(FPA)Cl]Cl (**2**), the characteristic C≡C stretching vibration appears at 2199 cm^{-1} compared to 2211 cm^{-1} for non-coordinated FPA.

Cyclic voltammetry

Redox potentials obtained from the cyclic voltammetric data of the complexes and of their parent fragments are listed in Table 1. In CH_2Cl_2, at the scan rate range used, both complexes [Ru([14]aneS$_4$)(4-FP)Cl]Cl and [Ru([14]aneS$_4$)(FPA)Cl]Cl present two reversible redox couples, the less positive one assigned to the Fe$^{II/III}$ oxidation of the ferrocenyl moiety, and the other to the Ru$^{II/III}$ electron transfer of the [Ru([14]aneS$_4$)Cl]$^+$ subunit (Fig. 1). The peak separations, ΔE_p, for each redox couple, ranged from 65 to 80 mV in CH_2Cl_2, which under the present experimental conditions are representative of one-electron reversible processes.

Table 1 Electrochemical data in CH_2Cl_2 at room temperature[a]

	Fe$^{II/III}$			Ru$^{II/III}$		
Compound	E_{pa}	E_{pc}	$E_{1/2}$ (ΔE_p)	E_{pa}	E_{pc}	$E_{1/2}$ (ΔE_p)
4-FP[b]	—	—	360	—	—	—
1	421	348	384(73)	969	904	936(65)
FPA	420	349	384(71)	—	—	—
2	449	373	411(76)	1014	941	978(73)
3	—	—	—	997	917	957(80) 756(111)[c]
4[d]	—	—	—	1473	1335	1404(138)

[a] Potentials in mV *vs.* Ag/Ag$^+$; scan rate is 200 mV s^{-1}; $E_{1/2}$ values are the average of the anodic and cathodic peak potentials, and $\Delta E_p = E_{pa} - E_{pc}$. [b] From ref. 2, at 100 mV s^{-1} in CH_2Cl_2. [c] In MeCN. [d] The complex is insoluble in dichloromethane, voltammogram carried out in MeCN at 20 mV s^{-1}; presents quasi-reversible behaviour.

The $E_{1/2}$ values of the free ligands 4-FP and FPA are slightly lower (24–27 mV) than the $E_{1/2}$ values of the Fe$^{II/III}$ couple in the corresponding binuclear complexes. This is indicative of low electronic coupling between the two metal centres, iron(II) and ruthenium(II), through the rather long unsaturated linking units. Furthermore, there are no significant effects resulting from the decreased distance between the two metal centres, from FPA to 4-FP (the corresponding $E_{1/2}$ values differ only by 3 mV).

The co-ordination of ruthenium(II) by pyridine (complex **3**) results in a substantial cathodic shift of the Ru$^{II/III}$ $E_{1/2}$ values (*ca.* 650 mV) compared with the complex [Ru([14]aneS$_4$)(MeCN)$_2$]Cl$_2$ (**4**) (Table 1, for experiments carried out in MeCN), probably due to the strong electron-donating ability of the pyridine ligand. The same pattern is observed for other ruthenium(II) complexes containing the macrocyclic ligand [12]aneS$_4$ incorporating the monodentate N-donor ligand indazole,[20b] for which the observed $E_{1/2}$ value for Ru$^{II/III}$ was 566 mV (in MeCN). On the other hand, there is no substantial effect on the half-wave potential of the ruthenium metal centre as a result of the change in the co-ordination sphere, from the pyridine to the FP moiety ($E_{1/2}$ for compound **1** is *ca.* 20 mV less positive than that for compound **3**, Table 1, experiments carried out in CH_2Cl_2). Once again, this indicates low electronic communication between the two metal centres of the heterobimetallic complexes.

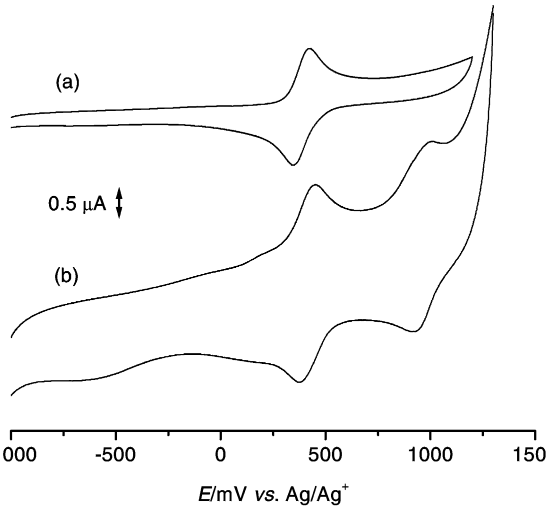

Fig. 1 Cyclic voltammograms for (a) FPA and (b) [Ru([14]aneS$_4$)(FPA)Cl]Cl (**2**) measured at 200 mV s^{-1} in CH_2Cl_2 with 0.1 M TBAPF$_6$.

Electronic absorption spectroscopy

The main absorption bands for compounds **1** and **2** appear in the ranges 250–300 and 330–360 nm, and in the visible region at 474 (**1**) and 444 nm (**2**) as pronounced shoulders (Table 2). The UV pattern is very similar to the electronic spectra of analogous Ru^{II} thioether polypyridyl complexes,[19,20] such as $[Ru([14]aneS_4)(L)Cl]X$ (L = monodentate nitrile ligand),[18] $[Ru([12]aneS_4)(L')]X_2$ (L′ = bidentate polypyridyl ligand)[20b] and other Ru^{II} compounds containing polypyridyl and S-donor ligands, or only polypyridyl ones.[25–30] The higher energy UV bands at 285–300 nm can be assigned to the intra-ligand $\pi \rightarrow \pi^*$ transitions of the pyridyl-containing ligands and to the ligand-to-metal charge transfer (LMCT) $(L) \rightarrow Ru(e_g^*)$.[20,27] For the bands at 330–360 nm, $Ru^{II}(dt_{2g}) \rightarrow \pi^*$ metal-to-ligand charge transfer (MLCT) would be expected, compared to other Ru^{II} analogues (Table 2).[20] However, these bands may strongly overlap with the CT bands $Fe(d\pi) \rightarrow Cp(\pi^*)$,[6,7b,28a] and make the individual assignment difficult. The referred $Ru^{II}(dt_{2g}) \rightarrow \pi^*$ MLCT bands are clearly observed for complexes where ferrocene is absent, *i.e.* $[Ru([12]aneS_4)(ind)Cl]Cl$ (363 nm) and $[Ru([14]aneS_4)(py)Cl]Cl$ (**3**) (402 nm) (Table 2). Complex **3** presents a good example for the strong bathochromic shift of the MLCT band due to the stabilisation caused by the lowering effect of the Ru^{2+} centre on the π orbital,[28b] which is also observed in cyclic voltammetry.

The broad band in the visible region at around 450 nm for compounds **1** and **2** corresponds to the Fe d–d transitions of the appended ferrocene.[4a,6,28a] In both cases there is neither a remarkable shift in wavelength nor a significant change in absorption coefficient compared to the free ligands.[6,11] From this point of view the influence of the Ru^{II} centre on ferrocene is weak or non-existent. It is also evident from these results that the ferrocene moieties have little influence on the ruthenium centre.

Thermogravimetric analysis

The complexes **1**–**2** and the corresponding precursor ligands 4-FP and FPA have been examined by TGA (Fig. 2). The yellow crystalline 4-ferrocenylpyridine is stable up to 135 °C but then melts and sublimes abruptly in the temperature range 135–240 °C (83.5% mass loss, DTG_{max} = 230 °C). A further 9.5% mass loss occurs on further heating to 360 °C. This second step may be an artefact arising from sublimation of material that had sublimed and recrystallised on colder parts of the thermobalance. The residual mass of 7% at 400 °C indicates that a small fraction of 4-FP decomposed during heating. The adduct $[Ru([14]aneS_4)(4\text{-}FP)Cl]Cl$ (**1**) decomposes in the temperature range 200–630 °C, leaving a residual mass of 28.5%. No clear step is observed that could be associated with the sublimation of the "free" ligand 4-FP. In fact, the degradation of the organometallic ligand and the Ru^{II} subunit occur in the same temperature range and are impossible to distinguish. Ferrocenyl-4-pyridylacetylene decomposes in several steps up to 780 °C, the onset of decomposition occurring at about 200 °C. The adduct $[Ru([14]aneS_4)(FPA)Cl]Cl$ (**2**) loses 12.5% mass in two steps up to 240 °C and then a further mass loss of 59% occurs in two steps up to 660 °C (DTG_{max} = 325, 430 °C). The residual mass at this temperature is the same as that for compound **1**.

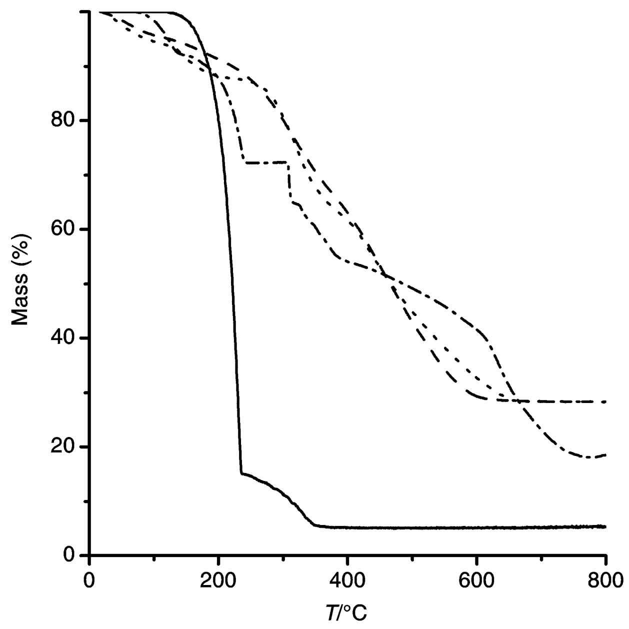

Fig. 2 TGA of 4-ferrocenylpyridine (solid line), $[Ru([14]aneS_4)(4\text{-}FP)Cl]Cl$ (**1**) (dashed line), ferrocenyl-4-pyridylacetylene (dashed-dotted line) and $[Ru([14]aneS_4)(FPA)Cl]Cl$ (**2**) (dotted line).

Table 2 UV/Vis absorption spectroscopic data measured in CH_2Cl_2 at room temperature

Compound	λ_{max}/nm ($\varepsilon \times 10^{-3}/M^{-1}\ cm^{-1}$)
4-FP[a]	454sh (0.63), 340 (2.11), 279 (12.40), 241 (17.20)
1	474sh (1.86), 360 (9.36), 274 (11.22)
FPA	449sh (0.76), 352 (2.32), 304 (12.80), 252 (13.70)
2	444sh (0.50), 359 (2.33), 303 (6.26), 248sh (9.98)
py	274 (0.16)
3	402sh (1.97), 351 (5.28), 268 (3.32)
$[Ru([12]aneS_4)(ind)Cl]Cl$	363 (0.36), 306 (0.38), 258 (0.81), 242 (1.00)[b]

[a] Data taken from ref. 6. [b] Relative intensities are given in parentheses.

Crystal structure of 1

The crystal structure of $[Ru([14]aneS_4)(4\text{-}FP)Cl]Cl$ (**1**) was determined by X-ray diffraction. Fig. 3 displays the molecular structure of the cation in **1** together with the numbering scheme used. This cation has a distorted *cis*-octahedral geometry with the equatorial plane formed by two macrocyclic sulfur

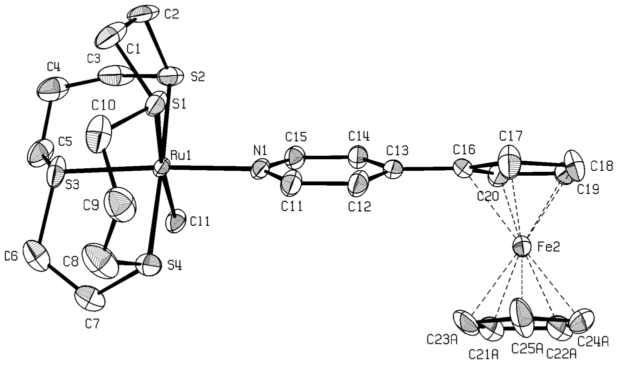

Fig. 3 View of the cation of **1** showing the labelling of the atoms. The cyclopentadienyl group with the lowest occupation factor has been omitted as have hydrogen atoms. Displacement ellipsoids are drawn at the 50% probability level. Selected bond distances (Å): Ru1–S1 2.276(1), Ru1–S2 2.339(1), Ru1–S3 2.305(1), Ru1–S4 2.336(1), Ru1–N1 2.131(4), Ru1–Cl1 2.448(1), Fe2–C16 2.036(4), Fe2–C17 2.025(5), Fe2–C18 2.023(5), Fe2–C19 2.033(4), Fe2–C20 2.0377(5), Fe2–C21A 1.971(12), Fe2–C22A 1.964(9), Fe2–C23A 2.054(10), Fe2–C24A 2.042(7), Fe2–C25A 2.096(7).

atoms (S1 and S3), one chlorine atom and one nitrogen atom from the FP ligand. The axial positions are occupied by the remaining two macrocyclic sulfur atoms (S2 and S4). The equatorial bond distances indicate that a *trans* effect is present in complex **1**, comparable with that reported for the complex [Ru([12]aneS$_4$)(ind)Cl]PF$_6$.[20b] Fe–C distances vary from 1.966(1) to 2.112(14) Å with a mean value of 2.055 Å. The [14]aneS$_4$ ligand is folded about the line through S2, Ru and S4, the plane of the pyridine ring bisects the S1–Ru–S4 angle and the cyclopentadienyl group is twisted 20° out of the plane of the pyridine. The S2–Ru–S4 angle [177.91(7)°] is close to the expected value of 180° for an ideal octahedron. The lack of coplanarity of the rings of the pyridylcyclopentadiene with each other and with RuS2 may partially explain the low electronic coupling observed. It is interesting to compare the structure of **1** with that of the square complex *cis*-[Pt^{II}(3-FP)$_2$Cl$_2$].[3] As found for **1**, each pyridine moiety in the platinum complex is not coplanar with the cyclopentadienyl ring to which it is covalently bonded. In the latter case, the angles between the two aromatic rings were 10.2 and 10.7°.

Conclusions

The DMSO adduct [Ru([14]aneS$_4$)(DMSO)Cl]Cl is a suitable starting material for the synthesis of ruthenium(II) thioether complexes containing monodentate pyridyl ligands, including ligands with an appended ferrocenyl moiety. By contrast, the analogous complex with ferroceneacetonitrile cannot be obtained in an analytically pure form. The heterobimetallic complexes [Ru([14]aneS$_4$)(L)Cl]Cl (L = 4-FP and FPA) exhibit low electronic communication between the metal centres. By comparison with the complexes [(4-FP)$_2$Re(CO)$_3$Cl][2] and *cis*-[Pt^{II}(3-FP)$_2$Cl$_2$][3] it is evident that the pyridine ring exerts a stopping effect on electronic interaction, possibly linked with the fact that the pyridyl and cyclopentadienyl rings are not coplanar. Work in our laboratory is in progress to investigate other conjugated pyridines as bridging units in binuclear ruthenium(II) thioether complexes.

Acknowledgements

This work was partly funded by FCT, POCTI and FEDER (Project PCTI/1999/QUI/32889). C. D. N. thanks the University of Aveiro for a grant. W. M. X. thanks the Bayerische Forschungsstiftung for a postdoctoral research associate fellowship. The authors are grateful to Prof. Dr. João Rocha (University of Aveiro) for generous support and access to research facilities.

References

1 *Ferrocenes*, eds. A. Togni and T. Hayashi, Wiley-VCH, Weinheim, 1994.

2 T. M. Miller, K. J. Ahmed and M. S. Wrighton, *Inorg. Chem.*, 1989, **28**, 2347.

3 O. Carugo, G. de Santis, L. Fabbrizzi, M. Licchelli, A. Monichino and P. Pallavicini, *Inorg. Chem.*, 1992, **31**, 765.

4 (*a*) T. Y. Liu, Y. J. Chen, C. C. Tai and K. S. Kwan, *Inorg. Chem.*, 1999, **38**, 674; (*b*) Y. J. Chen, C. H. Kao, S. J. Lin, C. C. Tai and K. S. Kwan, *Inorg. Chem.*, 2000, **39**, 189.

5 E. M. Barranco, O. Crespo, M. C. Gimeno, P. G. Jones, A. Laguna and M. D. Villacampa, *J. Organomet. Chem.*, 1999, **592**, 258.

6 W.-M. Xue and F. E. Kühn, *Eur. J. Inorg. Chem.*, 2001, 2041.

7 (*a*) B. Farlow, T. A. Nile and J. L. Walsh, *Polyhedron*, 1993, **12**, 2891; (*b*) K. Hutchison, J. C. Morris, T. A. Nile, J. L. Walsh, D. W. Thompson, J. D. Petersen and J. R. Schoonover, *Inorg. Chem.*, 1999, **38**, 2516.

8 L. F. Tang, W. L. Jia, Z. H. Wang, J. F. Chai and J. T. Wang, *J. Organomet. Chem.*, 2001, **637**, 209.

9 (*a*) J. T. Lin, S.-S. Sun, J. J. Wu, L. Lee, K.-J. Lin and Y. F. Huang, *Inorg. Chem.*, 1995, **34**, 2323; (*b*) J. T. Lin, S.-S. Sun, J. J. Wu, Y. C. Liaw and K.-J. Lin, *J. Organomet. Chem.*, 1996, **517**, 217; (*c*) J. T. Lin, M. F. Yang, C. T. Tsai and Y. S. Wen, *J. Organomet. Chem.*, 1998, **564**, 257.

10 W.-M. Xue, F. E. Kühn, E. Herdtweck and Q. Li, *Eur. J. Inorg. Chem.*, 2001, 213.

11 A. M. Santos, F. E. Kühn, W.-M. Xue and E. Herdtweck, *J. Chem. Soc., Dalton Trans.*, 2000, 3570.

12 I. S. Lee, S. S. Lee, Y. K. Chung, D. Kim and N. W. Song, *Inorg. Chim. Acta*, 1998, **279**, 243.

13 O. Briel, K. Sünkel, I. Krossing, H. Nöth, E. Schmälzlin, K. Meerholz, C. Bräuchle and W. Beck, *Eur. J. Inorg. Chem.*, 1999, 483.

14 (*a*) S. Sakanishi, D. A. Bardwell, S. Couchman, J. C. Jeffery, J. A. McCleverty and M. D. Ward, *J. Organomet. Chem.*, 1997, **528**, 35; (*b*) M. M. Bhadbhade, A. Das, J. C. Jeffery, J. A. McCleverty, J. Badiola and M. D. Ward, *J. Chem. Soc., Dalton Trans.*, 1995, 2769

15 J. T. Lin, J. J. Wu, C.-S. Li, Y. S. Wen and K.-J. Lin, *Organometallics*, 1996, **15**, 5028.

16 W. Y. Wong and W. T. Wong, *J. Chem. Soc., Dalton Trans.*, 1996, 3209.

17 J. A. Mata, E. Peris, S. Uriel, R. Llusar, I. Asselberghs and A. Persoons, *Polyhedron*, 2001, **20**, 2083.

18 M. Pillinger, I. S. Gonçalves, A. D. Lopes, J. Madureira, P. Ferreira, A. A. Valente, T. M. Santos, J. Rocha, J. F. S. Menezes and L. D. Carlos, *J. Chem. Soc., Dalton Trans.*, 2001, 1628.

19 J. Madureira, T. M. Santos, B. J. Goodfellow, M. Lucena, J. P. de Jesus, M. G. Santana-Marques, M. G. B. Drew and V. Félix, *J. Chem. Soc., Dalton Trans.*, 2000, 4422.

20 (*a*) S. Roche, H. Adams, S. E. Spey and J. A. Thomas, *Inorg. Chem.*, 2000, **39**, 2385; (*b*) T. M. Santos, B. J. Goodfellow, J. Madureira, J. P. de Jesus, V. Félix and M. G. B. Drew, *New J. Chem.*, 1999, **23**, 1015.

21 I. P. Evans, A. Spencer and G. Wilkinson, *J. Chem. Soc., Dalton Trans.*, 1973, 204.

22 Siemens, SMART, SAINT and XPREP Area-Detector Control and Integration Software, Siemens Analytical X-ray instruments Inc., Madison Wisconsin, USA, 1995.

23 G. S. Pawley, *Adv. Struct. Res.*, 1971, **4**, 1.

24 V. Shomaker and K. N. Trueblood, *Acta Crystallogr., Sect. B*, 1968, **24**, 63.

25 A. Das, H. C. Bajaj and M. M. Bhadbhade, *J. Organomet. Chem.*, 1997, **544**, 55.

26 M. J. Root, B. Patrick Sullivan, T. J. Meyer and E. Deutsh, *Inorg. Chem.*, 1985, **24**, 2731.

27 V. Balzani, A. Juris, M. Venturi, S. Campagna and S. Serroni, *Chem. Rev.*, 1996, **96**, 759.

28 (*a*) N. Chabert-Couchouron, C. Marzin and G. Tarrago, *New J. Chem.*, 1997, **21**, 355; (*b*) N. Chabert, L. Jacquet, C. Marzin and G. Tarrago, *New J. Chem.*, 1995, **19**, 443.

29 J.-Z. Wu, B.-H. Ye, L. Wang, L.-N. Ji, J.-Y. Zhou, R.-H. Li and Z.-Y. Zhou, *J. Chem. Soc., Dalton Trans.*, 1997, 1395.

30 B. J. Coe, S. Hayat, R. L. Bedoes, M. Helliwell, J. C. Jeffery, S. R. Batten and P. S. White, *J. Chem. Soc., Dalton Trans.*, 1997, 591.